Supplementary Information

Mechanism of cycling degradation and strategy to stabilize nickel-rich cathode

Xuerui Yang[a,1], Jiawei Chen[a,1], Qinfeng Zheng[a], Wenqiang Tu[a], Lidan Xing[a,b], Youhao Liao[a,b], Mengqing Xu[a,b], Qiming Huang[a,b], Guozhong Cao[c,*], Weishan Li[a,b,*]

a. School of Chemistry and Environment, South China Normal University, Guangzhou 510006, China.

b. Engineering Research Center of MTEES (Ministry of Education), Research Center of BMET (Guangdong Province), Engineering Lab. of OFMHEB (Guangdong Province), Key Lab. Of ETESPG (GHEI), and Innovative Platform for ITBMD (Guangzhou Municipality), South China Normal University, Guangzhou 510006, China.

c. Department of Materials Science and Engineering, University of Washington, Seattle, Washington 98195, United States.

* Corresponding authors, email: gzcao@u.washington.edu; liwsh@scnu.edu.cn.

Table S1

The solubility of some fluorides (g/100 ml water)*

Fluorides	**LiF**	**NiF_2**	**CoF_2**	**AlF_3**	**MnF_2**
Solubility	0.16	2.56	1.36	0.67	10.6

* W. F. Linke and A. Seidell, Am. Chem. Soc., 4th edn, 1966, vol. 2.

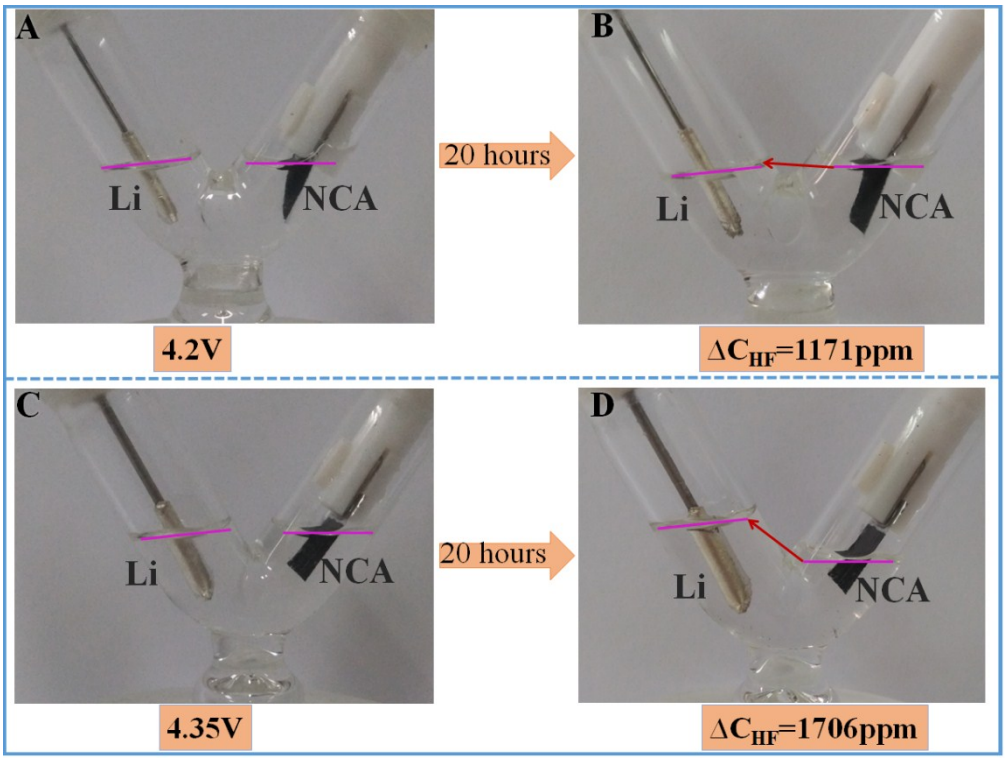

Fig S1. Li/NCA V-type cells: fresh (A, C) and after potential sweep at a scan rate of 0.01 mV s^{-1} from 3.0 V to 4.2 V (B) and to 4.35 V (D) and then kept at these potentials for 20 hours.

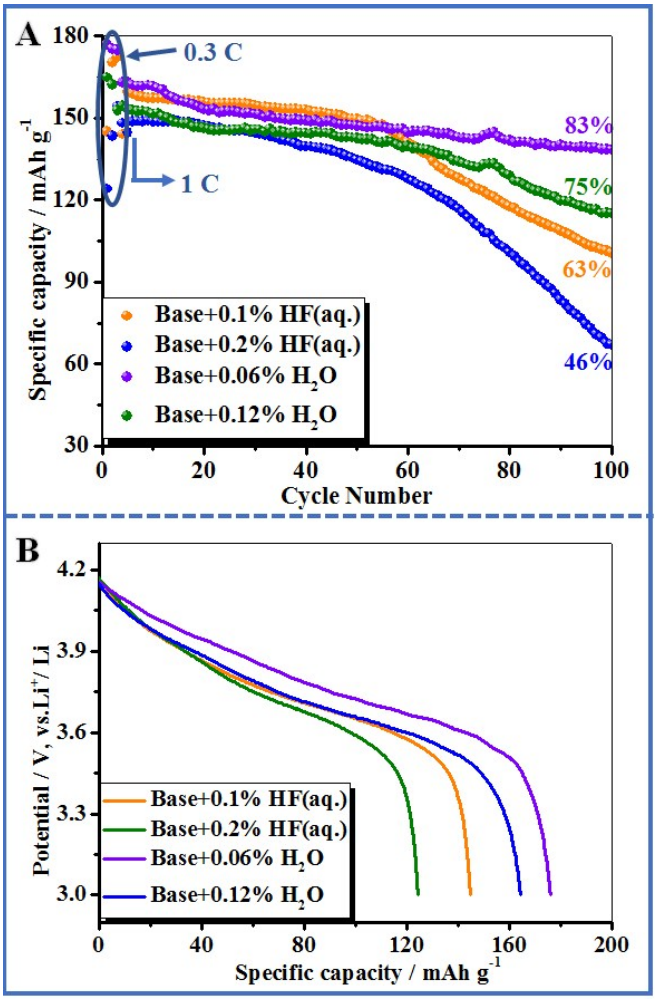

Fig S2. Cycling stability (A) of NCA in the base electrolyte with adding H_2O and HF (aq.) at 0.3 C for initial three cycles and at 1 C for subsequent cycles between 3.0 and 4.2 V and corresponding initial discharge curves (B).

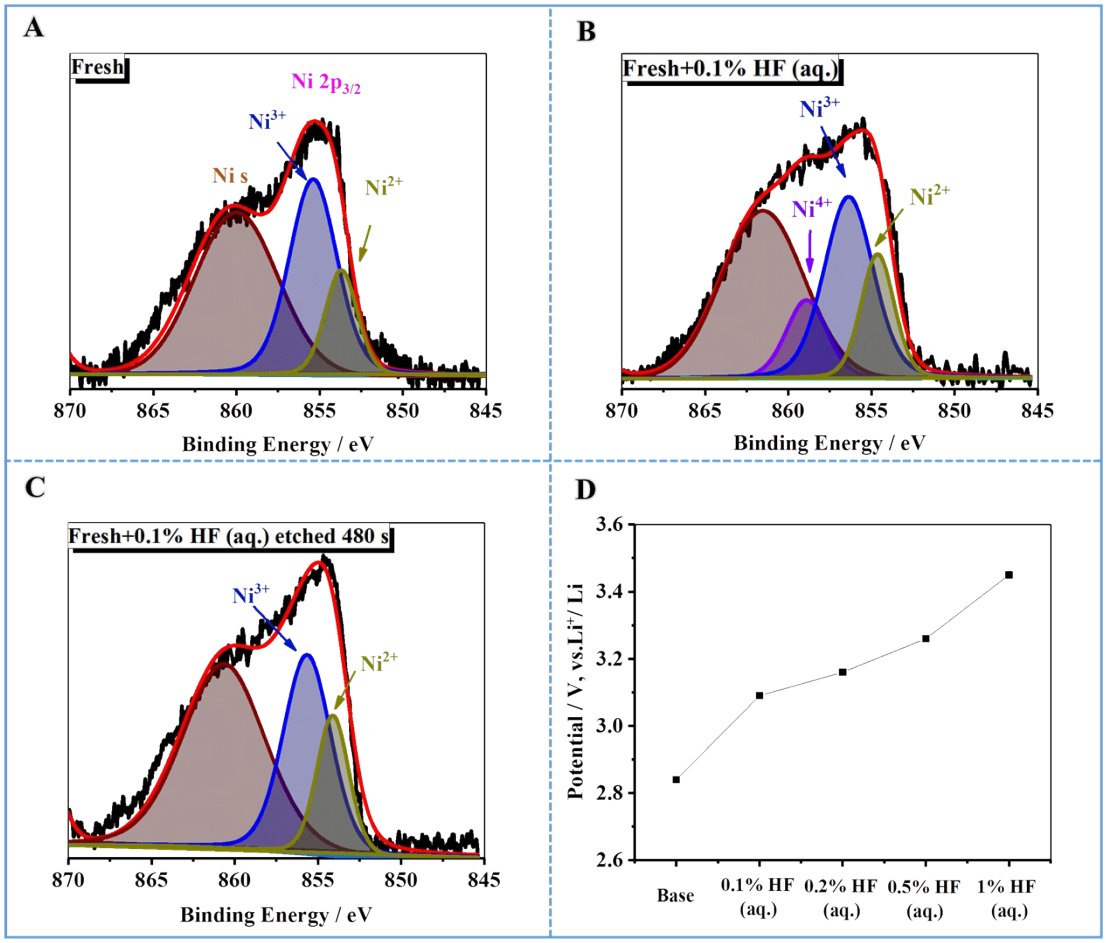

Fig S3. XPS patterns of NCA: fresh electrode (A); the electrode after immersion in 0.1% HF (aq.)-containing electrolyte for 50 h under room temperature without (B) and with Ar-ion sputtering for 480 s (C). Open circuit potential of NCA electrode after immersion in various HF (aq.)-containing electrolytes for 12 h (D).

Table S2

The photoelectron peak parameters of the samples in Fig S3.

		Ni^{2+}			Ni^{3+}			Ni^{4+}		
		FWHM / eV	**Position / eV**	**Intensity / cps**	**FWHM / eV**	**Position / eV**	**Intensity / cps**	**FWHM / eV**	**Position / eV**	**Intensity / cps**
Fresh	**$Ni2p_{3/2}$**	2.3	854.0	2500.6	3.0	855.7	6569.9			
Fresh + 0.1%HF(aq.)	**$Ni2p_{3/2}$**	2.3	854.6	3350.4	3.0	856.2	5796.8	2.9	858.9	2251.5
Fresh + 0.1%HF(aq.) etched 480s	**$Ni2p_{3/2}$**	2.3	854.1	2820.3	3.0	855.7	7200.0			

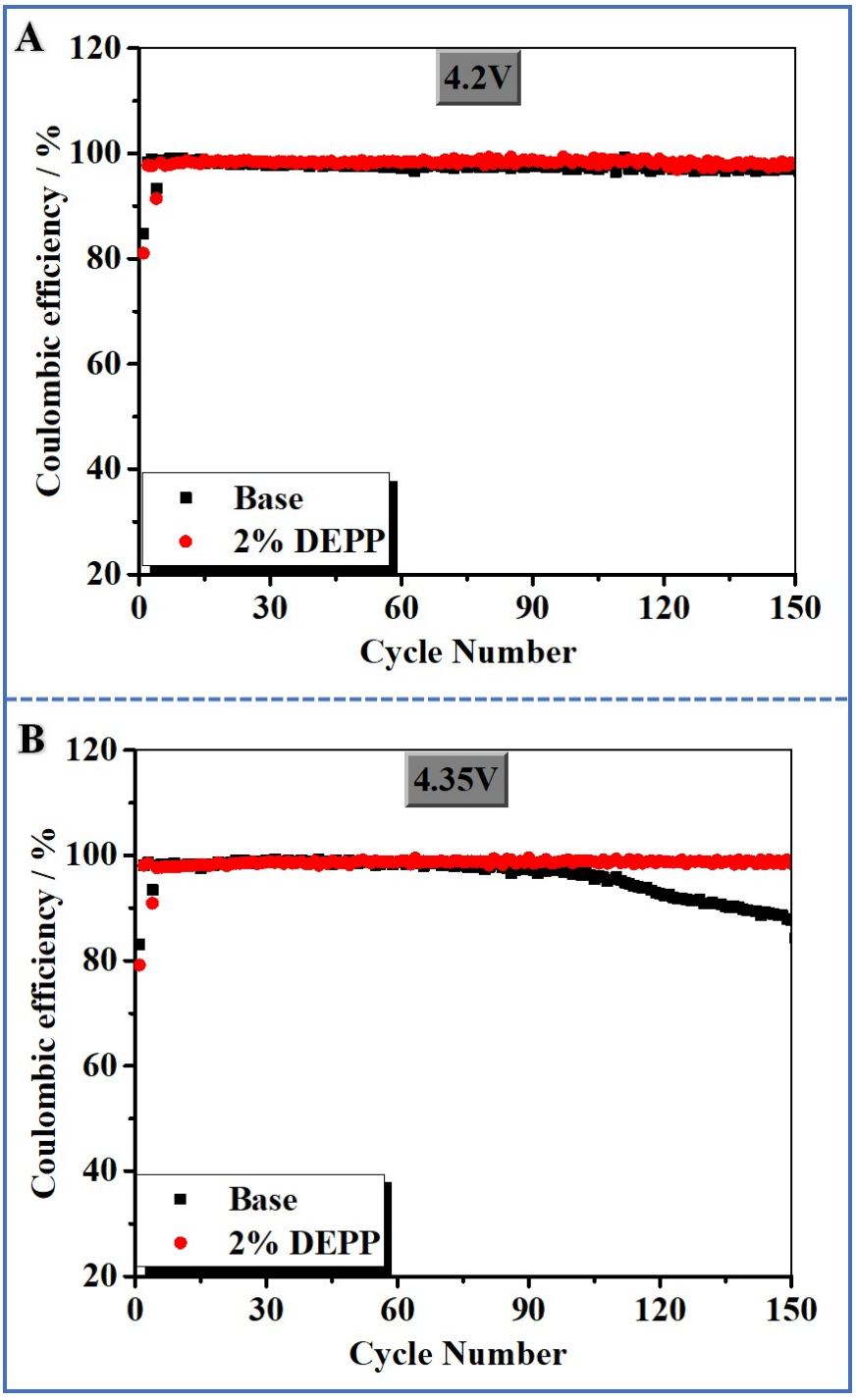

Fig S4. Coulombic efficiencies of Li/NCA cells cycled at 0.3 C for initial three cycles and at 1 C for subsequent cycles in the potential range of 3.0-4.2 V (A) and 3.0-4.35 V (B).

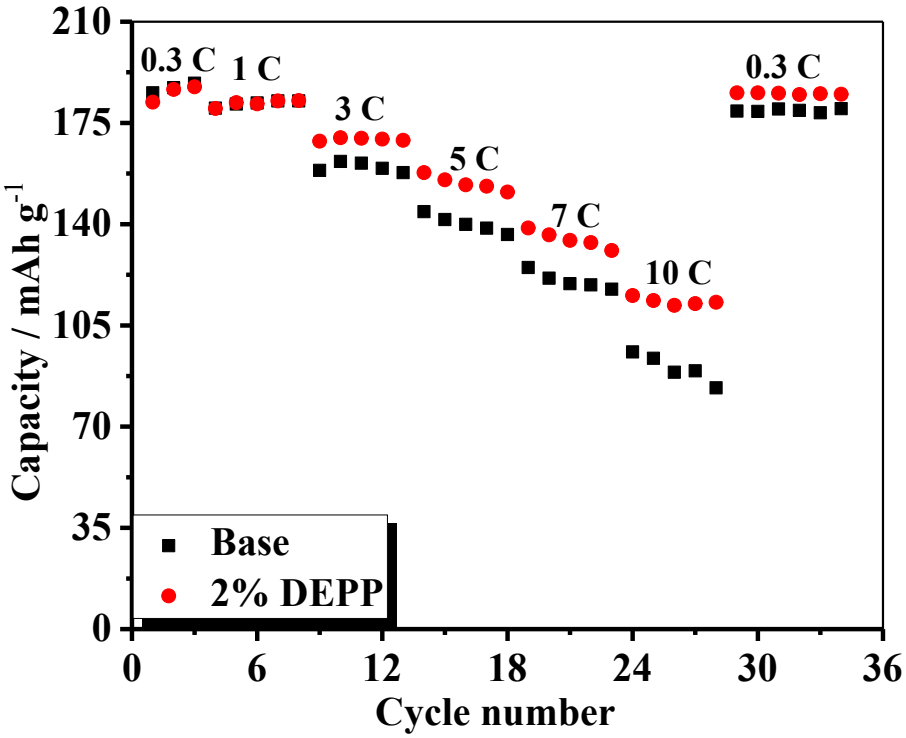

Fig S5. Rate capability of NCA electrodes in base and DEPP-containing electrolytes under room temperature.

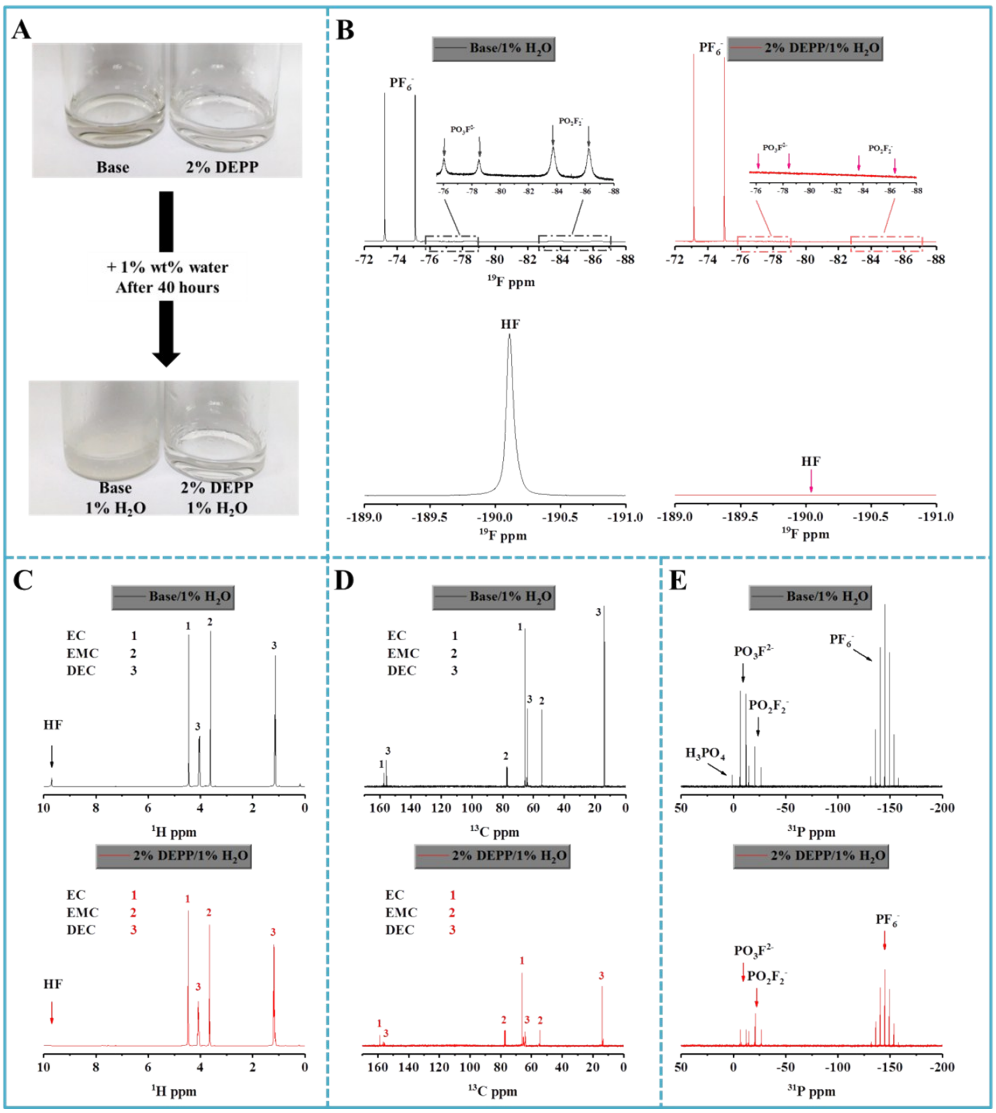

Fig S6. The base and 2% DEPP-containing electrolytes with 1 wt% water before and after storage at room temperature for 40h (A). ^{19}F (B), ^{1}H (C), ^{13}C (D) and ^{31}P (E) NMR spectra of 1 wt% water-containing base electrolytes with and without 2wt% DEPP after storage under room temperature for 40h.

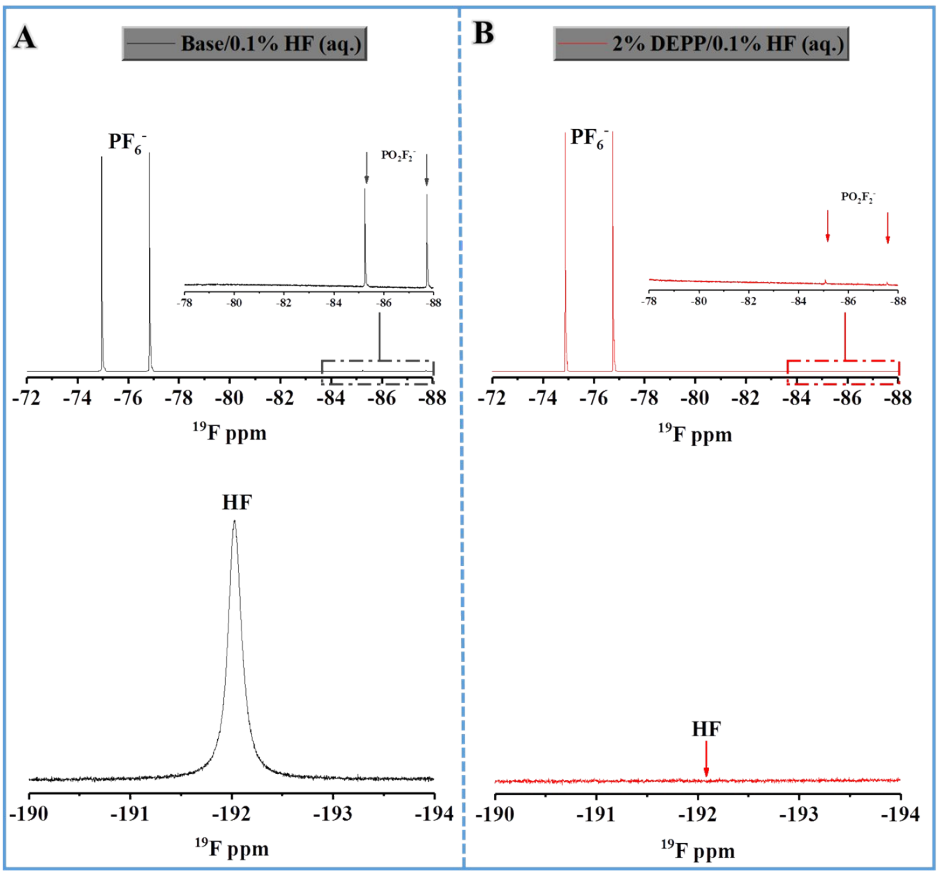

Fig S7. ^{19}F NMR spectra of 0.1% HF (aq.)-containing electrolytes with and without adding 2% DEPP.

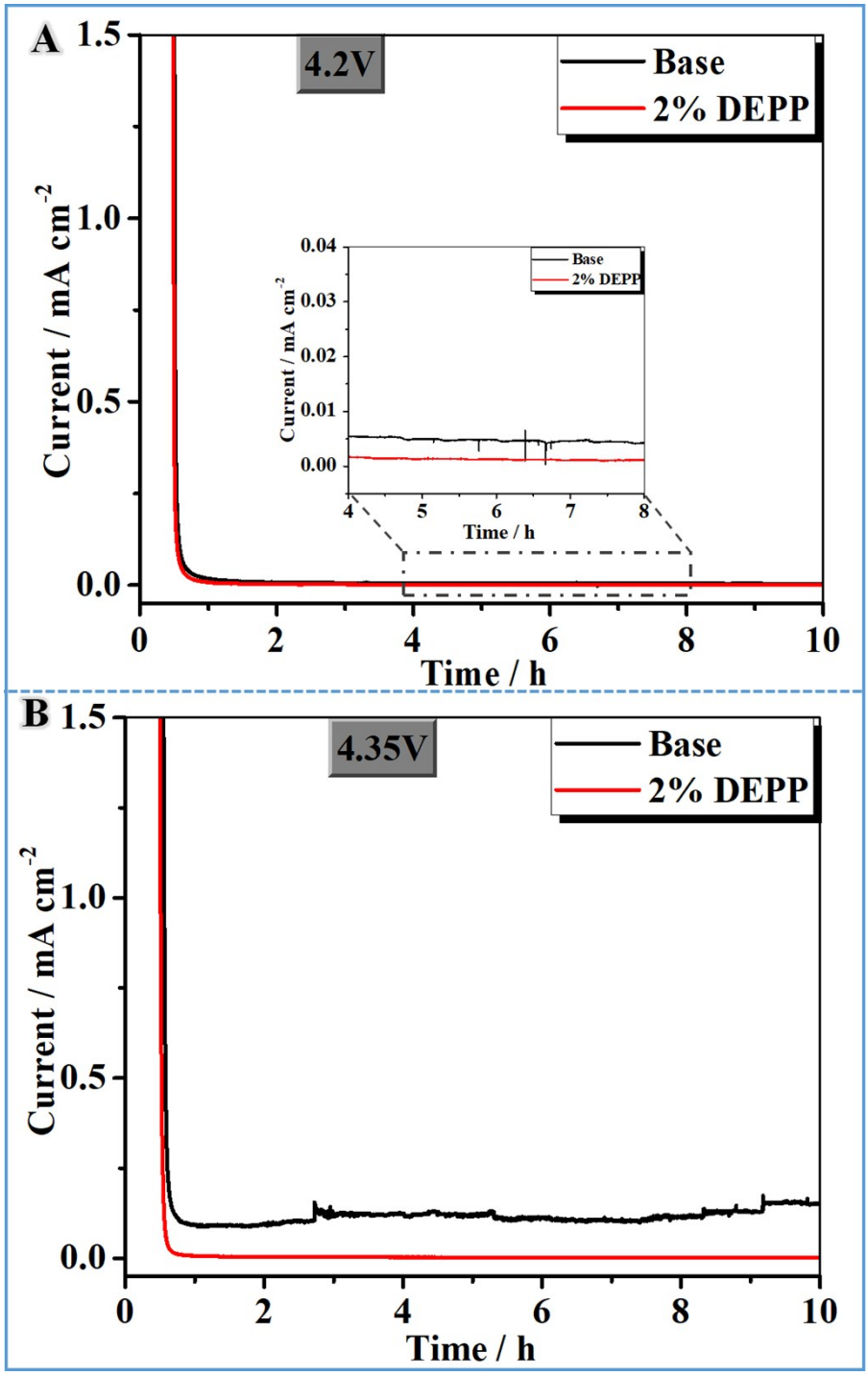

Fig S8. Chronoamperometric profiles of NCA electrodes in base and DEPP-containing electrolytes, obtained by charging/discharging Li/NCA coin cells at 0.3 C for three cycles under 4.2 (A) or 4.35 V (B) and then kept at upper charging voltages for 10 h.

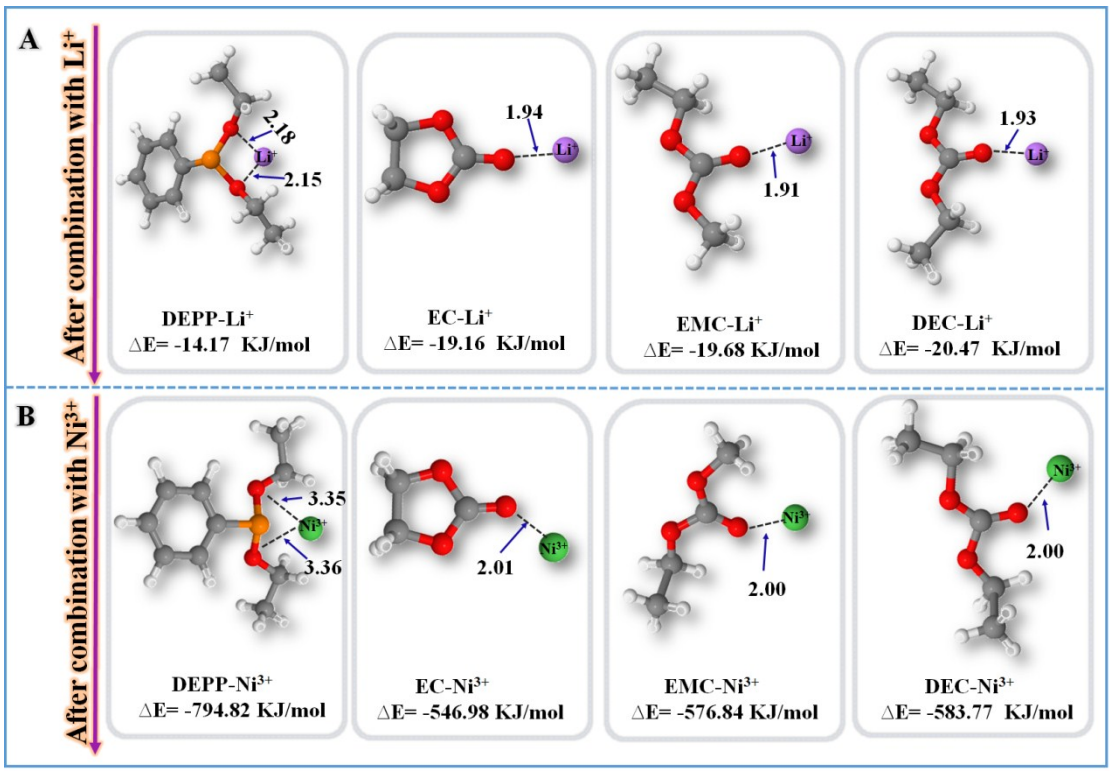

Fig S9. Optimized structures and the relative combination energies (ΔE, KJ mol^{-1}) between Li^+/Ni^{3+} and solvents or electrolyte additive: DEPP/EC/EMC/DEC-Li^+ (A) and DEPP/EC/EMC/DEC-Ni^{3+} (B).

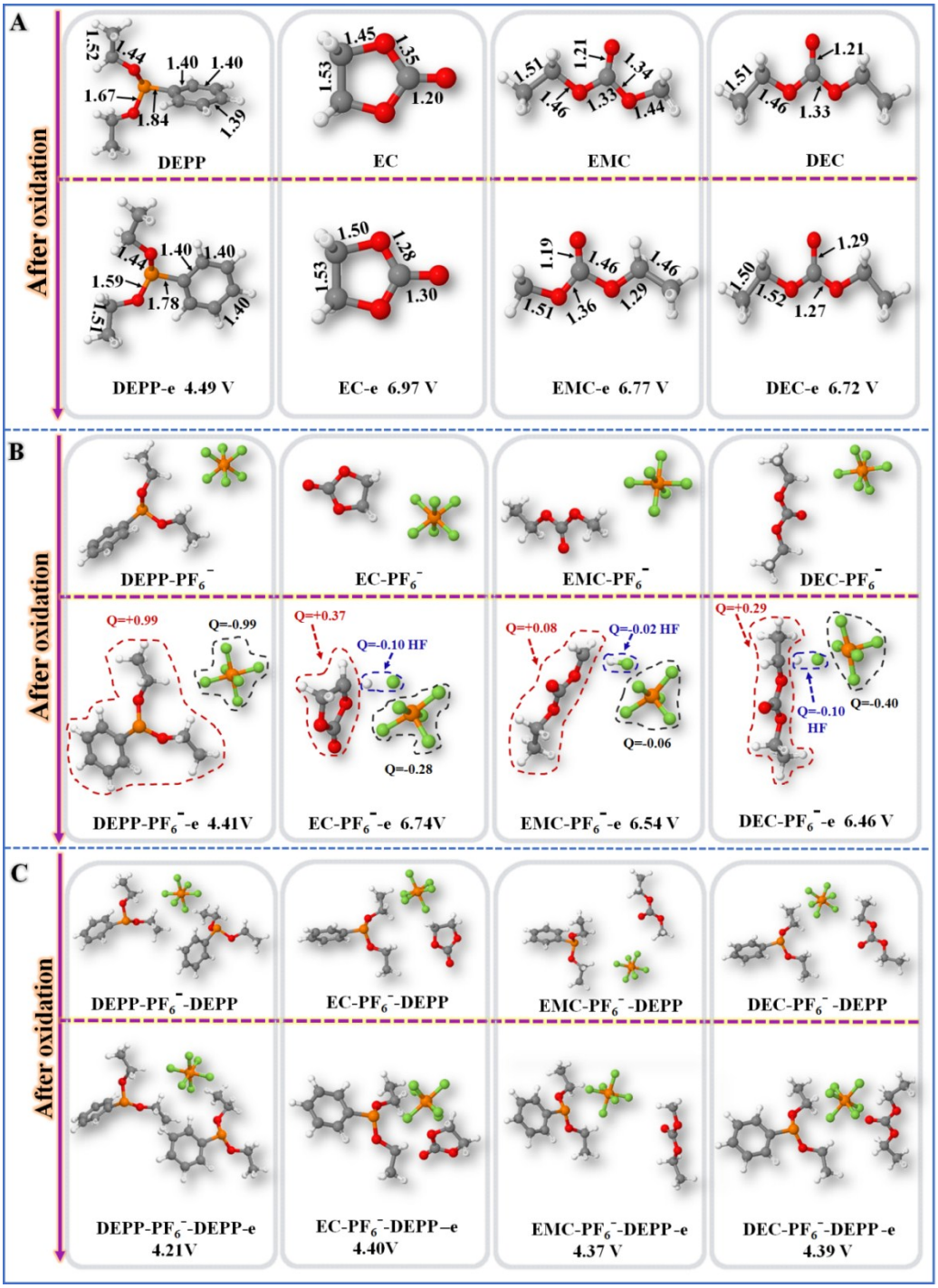

Fig S10. Optimized structures of DEPP, solvent molecules (EC, EMC, and DEC), DEPP-PF_6^-, solvent-PF_6^-, DEPP-PF_6^--DEPP, and solvent-PF_6^--DEPP before and after one electron oxidation (-e), together with the calculated oxidation potentials (V vs. Li^+/Li).

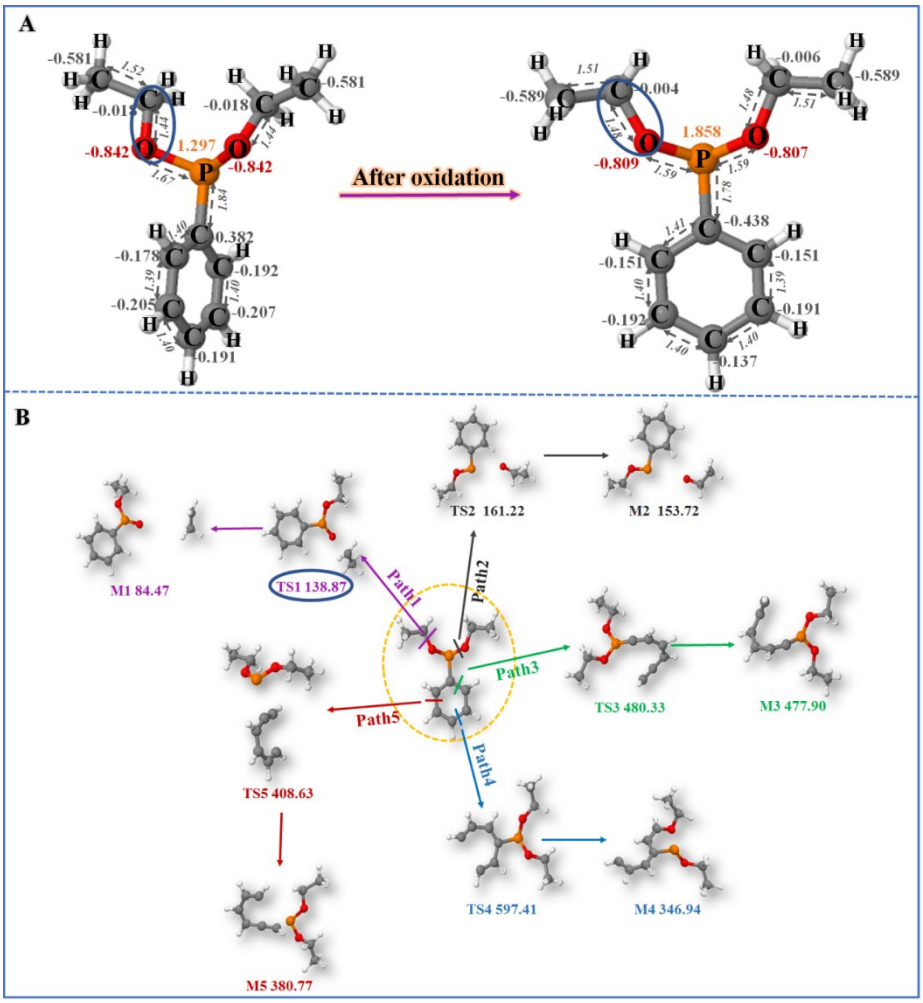

Fig S11. Optimized structure and NPA charge distributions of DEPP before and after one electron oxidation (A); Possible reaction pathways for the oxidation decomposition of DEPP and relative Gibbs free energy of all stationary points (B).

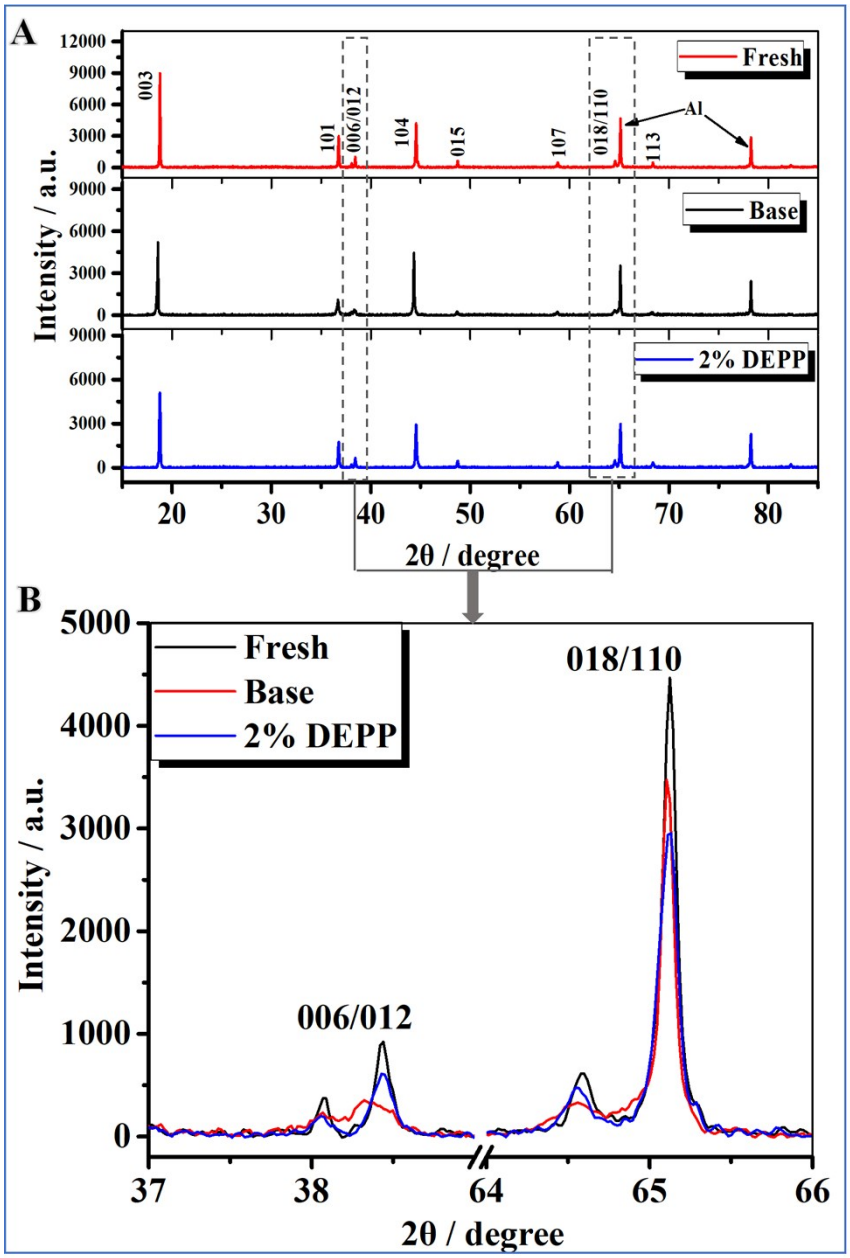

Fig S12. XRD patterns of NCA after 150 cycles in base and DEPP-containing electrolytes with a comparison of fresh one.

Table S3

Structural parameters of fresh and cycled NCA in base and 2% DEPP-containing electrolytes

Sample	Fresh	Base	2% DEPP
$I_{(003)}/I_{(104)}$	2.13	1.18	1.74
R-factor	0.47	0.56	0.49

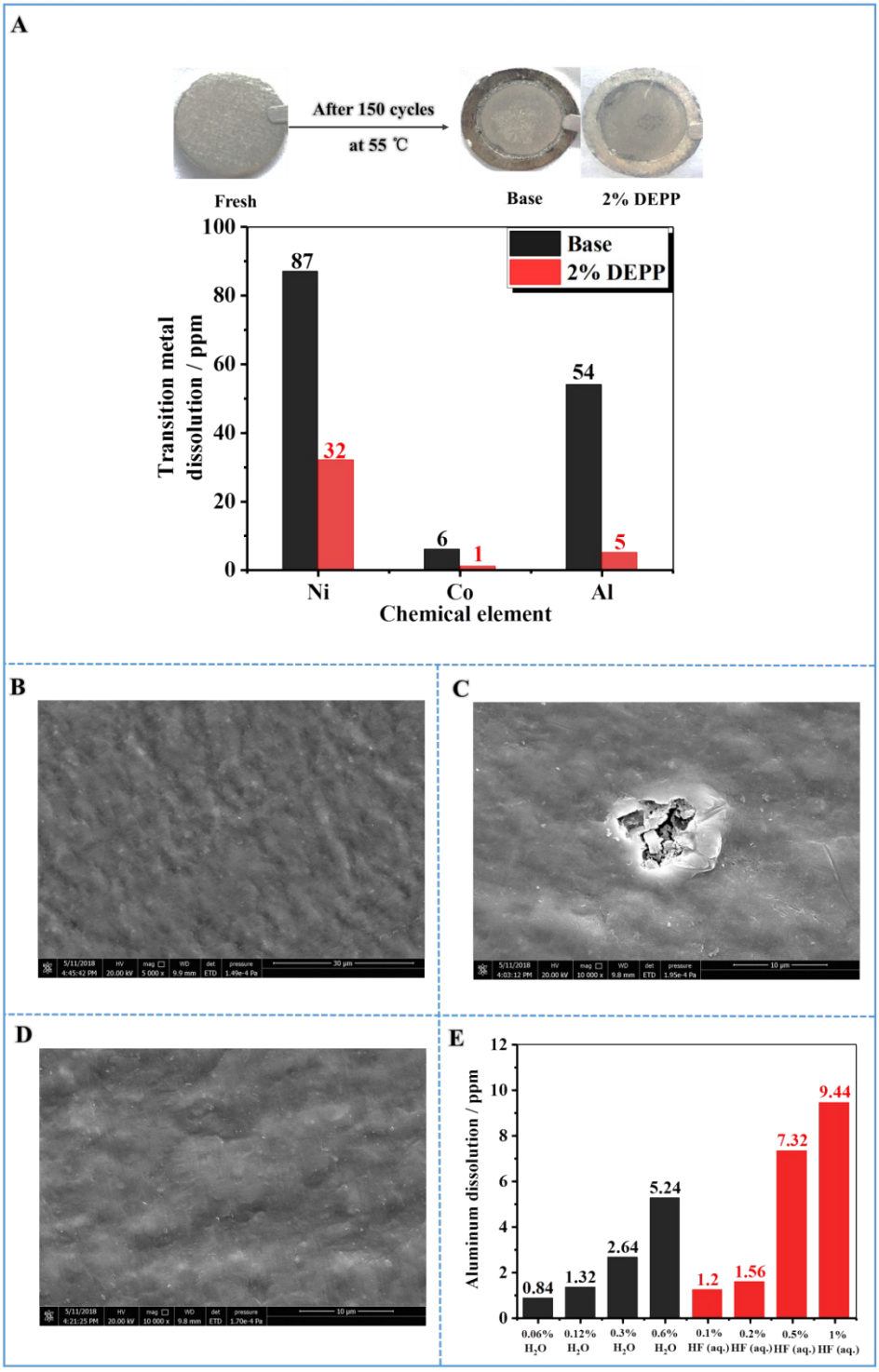

Fig S13. Contents of transition metal ions on lithium electrodes from the Li/NCA cells after 150 cycles in base and DEPP-containing electrolytes under room temperature (A). SEM images of fresh Al current collector (B) and the collectors after cycling in base (C) and DEPP-containing (D) electrolytes. Contents of Al in the H_2O and HF (aq.)-containing electrolytes after immersions of Al current collector for 50 h (E).

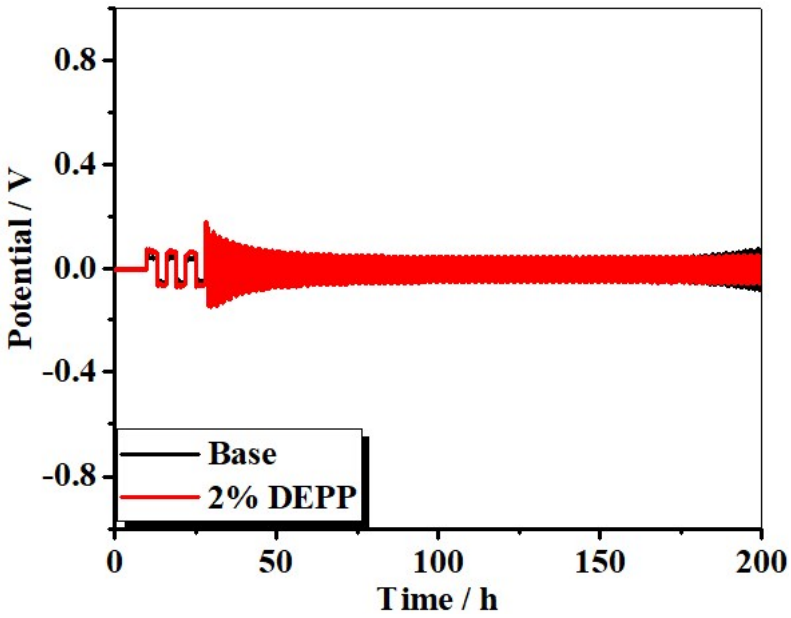

Fig S14. Voltage profiles of the Li/Li symmetric cells during the stripping-plating test at a current density of 0.84 mA/cm^2 after 0.25 mA/cm^2 for the first three cycles in base and DEPP-containing electrolytes.